IEEE Access
Multidisciplinary ⁝ Rapid Review ⁝ Open Access Journal

Received June 17, 2021, accepted June 28, 2021, date of publication July 5, 2021, date of current version July 15, 2021.

Digital Object Identifier 10.1109/ACCESS.2021.3094736

L-Shape Propagated Array Configuration With Dynamic Reconfiguration Algorithm for Enhancing Energy Conversion Rate of Partial Shaded Photovoltaic Systems

A. SRINIVASAN[1], (Member, IEEE), S. DEVAKIRUBAKARAN[1],
B. MEENAKSHI SUNDARAM[1], PRAVEEN KUMAR BALACHANDRAN[2],
SANTHAN KUMAR CHERUKURI[3], D. PRINCE WINSTON[4], (Member, IEEE),
THANIKANTI SUDHAKAR BABU[5,6], (Senior Member, IEEE),
AND HASSAN HAES ALHELOU[7,8], (Senior Member, IEEE)
[1]Department of Electrical and Electronics Engineering (EEE), Sethu Institute of Technology, Virudhunagar, Tamil Nadu 626115, India
[2]Department of Electrical and Electronics Engineering (EEE), Bharat Institute of Engineering and Technology, Hyderabad, Telangana 501510, India
[3]Department of Electrical and Electronics Engineering (EEE), Lords Institute of Engineering and Technology, Hyderabad, Telangana 500091, India
[4]Department of Electrical and Electronics Engineering (EEE), Kamaraj College of Engineering and Technology, Madurai, Tamil Nadu 626001, India
[5]Department of Electrical and Electronics Engineering, Chaitanya Bharathi Institute of Technology, Hyderabad, Telangana 500075, India
[6]Department of Electrical and Electronics Engineering, Nisantasi University, 34398 Istanbul, Turkey
[7]Department of Electrical Power Engineering, Faculty of Mechanical and Electrical Engineering, Tishreen University, Lattakia, Syria
[8]School of Electrical and Electronic Engineering, University College Dublin, Dublin 4, D04 V1W8 Ireland

Corresponding author: Hassan Haes Alhelou (alhelou@ieee.org) and S. Devakirubakaran (kirubathas@gmail.com)

This work was supported in part by the Department of Science and Technology, India, under Grant DST/TMD/SERI.

ABSTRACT Partial shading is an unavoidable factor that reduces the performance of solar PV systems. The PV system receives uneven irradiation due to partial shading which causes the mismatch loss. The partial shading distracts the irradiation from the PV modules that makes the healthy modules as idle or low performing modules. The mismatch loss can be mitigated by uniformly distributing the partial shading over the PV array. In this work, L-shaped propagated array configuration method with a new dynamic reconfiguration algorithm have proposed for enhancing the energy conversion under the partial shading conditions. A new kind of array configuration is implemented in a 4 × 4 PV array for the better shade dispersion. Further, a dynamic reconfiguration algorithm is employed to disperse the effect of partial shading. The combination of new array configuration and reconfiguration method is simulated in MATLAB/Simulink®and implemented in hardware. The outputs are measured under all possible shading patterns and validated with the outputs of convention methods for observing the enhanced energy conversion rate of the proposed system.

INDEX TERMS Array configuration, futoshiki puzzle pattern, mismatch loss, partial shading, PV array reconfiguration, total cross tied (TCT), sudoku pattern.

I. INTRODUCTION

Photovoltaic (PV) system accelerates its development in the global energy market in recent years because of its eco-friendly characteristics, reliability and renewability [1], [2]. Many countries prefer the solar PV plant for future energy demand. The structure of a PV cell is made with the bonding of n-type and p-type semiconductors with a PN-junction. The energy of photons in the sunlight breaks the bonding electrons in n-type and makes it flow to the load by through the p-type. The amount of free electrons liberated by the photons is the actual amount of current generated by the PV cell [3]. Some environmental factors like partial shading due to clouds, shadows of nearby objects, dust accumulation, dropping of birds, etc., will distract the rate of incident photons, which directly reduces current generation [4], [5]. The partial shading distributes non-uniform irradiation over the PV array which causes the mismatch losses. The power generation by the un-shaded PV cell will not be available at the load because of the shaded PV cells is the effect of

The associate editor coordinating the review of this manuscript and approving it for publication was Nagesh Prabhu.

This work is licensed under a Creative Commons Attribution 4.0 License. For more information, see https://creativecommons.org/licenses/by/4.0/

mismatch loss [6], [7]. The non-uniform distribution of the shading causes multiple peaks with multiple local maximum power points (LMPP) in the P-V and I-V characteristics of the PV array. Many approaches were proposed to obtain the maximum power from the partial shaded PV array.

Bypass diode configuration is one of the earlier techniques to suppress the effect of partial shaded cell within it. At normal conditions, the internal resistance of the PV cell is lesser than the bypass diode. At partial shading conditions, the internal resistance of the PV cell is increased more than the bypass diode. So the current flows through the low resistance path of the diode. The bypass diodes will not allow the shaded cell to limit the current generation of the non-shaded PV cells and different approaches for using a bypass diode configuration is given in [8].

The global maximum power point (GMPP) is tracked and obtained from the various LMPP by incorporating the MPPT algorithm with the controller. The main concept of the MPPT algorithm is to maintain the resistance of source and load to be equal or approximately equal. The Perturb & Observe (P&O) algorithm [9], Incremental conductance (InC) algorithm [10] are the conventional MPPT algorithm used in the early days. In recent days, many types of MPPT algorithms are proposed in [11] by using the soft computing optimization techniques like artificial neural network (ANN), Particle swarm optimization (PSO), ant colony optimization (ACO) and, etc. for enhancing the accuracy of tracking GMPP. The fractional chaos based flower pollination algorithm is proposed in [12] to enhance the power generation of PV array under varying partial shaded conditions. The reduced PV current and PV voltage due to partial shading is compensated by using the converters. But this work requires more number of converters and sensor which increase the installation and maintenance cost of the PV system. The various array configurations such as Series-Parallel (SP), Bridge Link (BL), Total Cross Tied (TCT), Sudoku Pattern, Futoshiki Puzzle Pattern (FPP) are proposed in [13], [14]. The TCT, BL, HC, Sudoku, and FPP are dispersing the shading effect over the PV array to change the uneven current generating rows into even current generating row, which increases the power output. The level of partial shading is unpredictable and the effectiveness of array configuration is dumped by the complicated shading patterns.

Dynamic array reconfiguration techniques [15], [16] are changing the interconnection between the PV modules to equally disperse the effect of shading. In [17], authors proposed an innovative reconfiguration via multi objective grey wolf optimizer to mitigate the partial shading effect. Further, comprehensive study on different population based PV reconfiguration is introduced in [18] with an aim of row current minimization. In [19], current injection-based configuration method is been proposed for minimizing the mismatch losses in the PV system. A current source is connected in parallel with each row of the PV array, and it compensates the distorted current to the row. This method requires n number of converters and measuring units for compensating the current with the rows. A two-step reconfiguration method is been proposed in [20], at where the reconfiguration process is done in two steps. The PV array dimension is varied in each step. In step one the PV array operates in its original array size and in second step the PV system alters into the new dimension of rows with half of the size and columns with doubled size. Normal array configuration limits shade dispersing rate of this technique for some shading patterns, Where the proposed array configuration has high resistivity to the partial shading effect. The reconfiguration technique requires more number of sensors, where the reconfiguration method used in this work requires less number of sensors. In this work, L-shaped array configuration with dynamic reconfiguration method is proposed for uniformly dispersing all kind of shading patterns. The proposed array configuration can disperse the maximum amount of shading in the PV array. The remaining shading effect in the PV array can be completely or nearly nullified by the dynamic reconfiguration algorithm. This array reconfiguration algorithm does not require more number of data or sensor like the existing electrical array reconfiguration techniques. The current measurement is the only required data for measuring the shade dispersion rate and performing the reconfiguration algorithm. A switching circuit is incorporated with the PV array is executing the reconfiguration pattern which is generated by the algorithm. The work is simulated in MATLAB/Simulink© and implemented in the hardware. The performance, shading dispersion rate, mismatch loss analysis and the percentage of error of the proposed work have been compared and analysed with the other configurations such as TCT, Sudoku, and FPP.

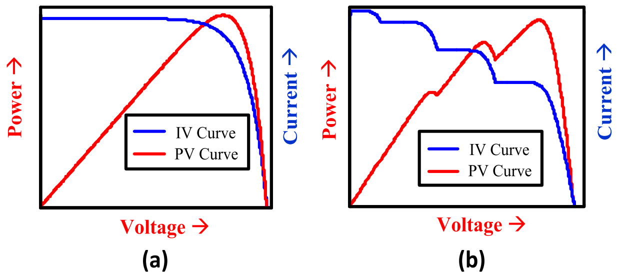

FIGURE 1. **P-V and I-V characteristics (a) Under uniform irradiation (b) Under partial shading.**

The rest of the paper is organized as follows. Section II presents the description of proposed array configuration and its structure. Section III presents the overview of the simulation, test models of the proposed configuration, the overall simulation flowchart and the results obtained from the simulation. Section IV summarizes and concludes the paper.

II. DESCRIPTION OF PROPOSED PV ARRAY CONFIGURATION

A. PROPOSED ARRAY CONFIGURATION

The sudoku and futoshiki array configurations are applicable only for the square PV arrays and for the non-square PV arrays its logics were failed. The proposed array configuration is perfectly suitable for squared PV arrays, non-squared PV array with odd number of columns. For the non-squared PV array with even number of columns, the configuration may produce PV rows with repeated PV modules with the optimized location. The proposed PV array is generated by forming the rows with propagation of L from the starting node and it continues till reaching the final column or the previous to it. When it reaches the final or previous column of the PV array, the L propagation should end there and started again from the second column of the PV row and it continues to the end, which selects one panel from every PV row and column. This frames the PV rows with distinct PV panels from each row or the repeated PV panels with the optimized distance. Starting node and its corresponding column is the factors to consider in the propagation. This array configuration greatly reduces the mismatch losses in the PV system as compared to sudoku. The L-shape propagation of each rows for the 4 × 4 PV array is shown in Fig.2.

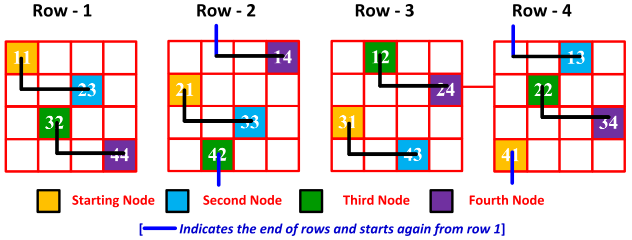

FIGURE 2. L-shape propagation diagram for the 4 × 4 PV array.

For executing the reconfiguration algorithm, the PV panels are coupled as the individual units as flexible unit and static unit. For the n × m PV array, (2n) numbers of PV groups are formed and each PV group consists of (m/2) number PV modules. For the square PV arrays the PV row has been split into two equal parts with (m/2) PV panels for the fixed and adaptive parts. For the non-square PV arrays, each row has been splitter into ((m/2)+1) numbers of panels for the fixed part and ((m/2)-1) numbers of panels in the adaptive part. Two PV groups are connected in parallel to forms the m number of rows with n number of PV modules in each row. Further, these rows are connected in series to create an n × m proposed array configuration. For the 4 × 4 PV array, eight number of PV groups framed with the dimension of 2 × 1. Two PV groups which have no repeated PV modules in the same row or on its corresponding column have been connected in parallel to create a row 4×1 array size. The array formation is completed with connecting four number of 4 × 1 PV arrays in series. The fig.3.(d) shows the group formation diagram from TCT by the L-shape propagation with grouping and the fig.3.(e) shows the matrix configuration diagram of the proposed array configuration.

B. RECONFIGURATION ALGORITHM

The reconfiguration algorithm gives the flexibility to the PV array to change its interconnection for equally disbursing

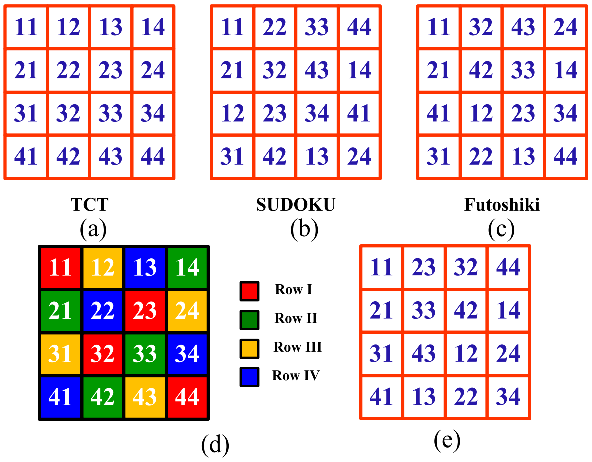
TCT

(a)

11	12	13	14
21	22	23	24
31	32	33	34
41	42	43	44

SUDOKU

(b)

11	22	33	44
21	32	43	14
12	23	34	41
31	42	13	24

Futoshiki

(c)

11	32	43	24
21	42	33	14
41	12	23	34
31	22	13	44

(d)

11	12	13	14
21	22	23	24
31	32	33	34
41	42	43	44

🟥 Row I
🟩 Row II
🟨 Row III
🟦 Row IV

(e)

11	23	32	44
21	33	42	14
31	43	12	24
41	13	22	34

FIGURE 3. (a) Matrix configuration diagram of TCT (b) matrix configuration diagram of Sudoku (c) matrix configuration diagram of FPP (d) Propagation of L for each rows (e) Matrix configuration diagram of L-shape propagated array configuration.

the partial shading over it. For executing the reconfiguration algorithm m × n PV array has been splitter into two units as static unit and flexible units with (m/2) × n each for PV array with even numbers of column or ((m/2)-1) × n and (m/2) × n for PV array with odd number of columns. Static and flexible units were connected through the switching circuits which is capable to connect any flexible unit with the static unit based on the current generation. So that, each PV row can generate even current that leads to the minimum mismatch losses between the PV rows. The functional block diagram and the functional circuit diagram of the proposed reconfiguration algorithm is shown in Fig.4. (a) and Fig.4. (b).

Various steps involved for executing the reconfiguration algorithm. The entire PV array is splitter into two units as static and flexible unit. A switching circuit is placed between these units for connecting them. Short circuit current measurement for each row of static part and flexible part is obtained. Based on the short circuit current, rows in flexible unit are connected with the rows of static unit through switching circuit. This switching operation completes the reconfiguration algorithm. After the switching PV array will be operated with the even current generating rows. This entirely reduces the mismatch losses from the PV system.

The short circuit current of each rows in static and flexible unit is obtained as the following expression (1) and (2)

$$I_{SCSU_{Ri}} = \left[I_{SCSU_{Ri}} \; I_{SCSU_{Ri}} \quad \cdots\cdots \quad I_{SCSU_{R(m-1)}} \quad I_{SCSU_{Ri}} \right] \tag{1}$$

$$I_{SCSU_{Ri}} = \left[I_{SCSU_{Ri}} \quad I_{SCSU_{Ri}} \quad \cdots\cdots \quad I_{SCSU_{R(m-1)}} \quad I_{SCSU_{Ri}} \right] \tag{2}$$

where, $I_{SCSU_{Ri}}$ is the short circuit current of static unit rows and $I_{SCFU_{Ri}}$ is the short circuit current of flexible unit rows.

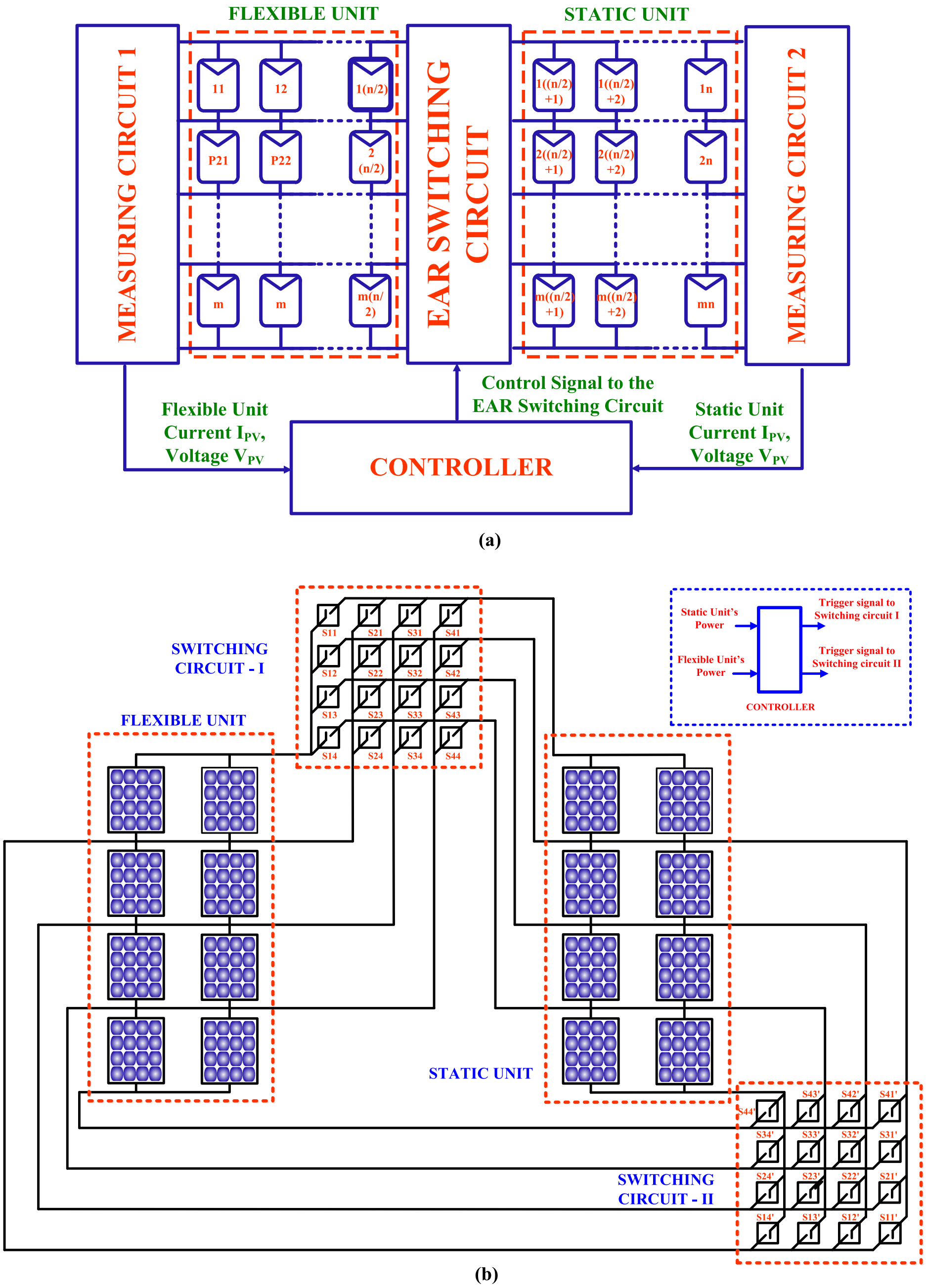
FLEXIBLE UNIT
STATIC UNIT
MEASURING CIRCUIT 1
EAR SWITCHING CIRCUIT
MEASURING CIRCUIT 2
11
12
1(n/2)
P21
P22
2 (n/2)
m
m
m(n/2)
1((n/2)+1)
1((n/2)+2)
1n
2((n/2)+1)
2((n/2)+2)
2n
m((n/2)+1)
m((n/2)+2)
mn
Flexible Unit Current I_{PV}, Voltage V_{PV}
Control Signal to the EAR Switching Circuit
Static Unit Current I_{PV}, Voltage V_{PV}
CONTROLLER
(a)
SWITCHING CIRCUIT - I
FLEXIBLE UNIT
S11
S21
S31
S41
S12
S22
S32
S42
S13
S23
S33
S43
S14
S24
S34
S44
Static Unit's Power
Flexible Unit's Power
Trigger signal to Switching circuit I
Trigger signal to Switching circuit II
CONTROLLER
STATIC UNIT
S44'
S43'
S42'
S41'
S34'
S33'
S32'
S31'
S24'
S23'
S22'
S21'
S14'
S13'
S12'
S11'
SWITCHING CIRCUIT - II
(b)

FIGURE 4. (a) Functional block diagram for mXn PV array (b) Functional circuit diagram of the proposed array reconfiguration scheme for 4 × 4 PV array.

The short circuit currents of static and flexible units is ranked as the following expression (3) and (4),

$$I_{SCSU_{Rsort}} = SORT_{\max}\left[I_{SCSU_{Ri}}\right] \tag{3}$$

$$I_{SCFU_{Rsort}} = SORT_{\min}\left[I_{SCFU_{Ri}}\right] \tag{4}$$

Static unit's short circuit current is ranked as maximum to minimum, whereas flexible unit's short circuit current is ranked as minimum to maximum. For the reconfiguration, Static unit's row with rank 1 should be connected to flexible unit's row with rank 1, i.e., the maximum power generating row of the static unit is connected with the minimum current generating row of the flexible unit.

$$I_{SC_{Ri}} = \left[I_{SCSU_{Rsort_i}} + I_{SCFU_{Rsort_i}}\right] \tag{5}$$

The output current will be obtained by using the following equation (6)

$$I_{out} = FillFactor \times \min(I_{SC_{Ri}}) \tag{6}$$

The dynamic reconfiguration algorithm for m × n PV array is performed by the following steps,

Step-1: Splits PV array into two units as static and flexible unit.
Step-2: Measures short circuit current of each rows static and flexible units
Step-3: Rank static unit's short circuit current from maximum to minimum
Step-4: Rank the flexible unit's short circuit current from minimum to maximum.
Step-5: Connect the flexible unit's minimum current generating row with the maximum current generating row of the static unit.
Step-6: Repeat the same with a regular time interval.

III. RESULTS AND DISCUSSION

The proposed hybrid reconfiguration method is compared with the existing configurations like (a) TCT, (b) Sudoku puzzle pattern and (c) Futoshiki Puzzle pattern under eight various shading patterns such as (i) uneven column shading (UC), (ii) Uneven Row shading (UR), (iii) Diagonal shading (DS), (iv) Random shading (RS), (v) Short and Narrow shading (SN), (vi) Short and Wide shading (SW), (vii) Long and narrow shading (LN) and (viii) Long and Wide shading (LW). Proposed array configuration with the conventional array configuration is analysed under the eight shading patterns. The percentage of error is also a factor calculated to measure the uniformity between the current generations of each row in the PV array. The difference between the maximum generating row and the minimum current generating row gives the percentage of error so that it can be said as healthy or faulty operating condition.

$$Percentage\_of\_Error = \left(\frac{I_{SC_{R\max}} - I_{SC_{R\min}}}{I_{SC_{R\max}}}\right) \times 100 \qquad (7)$$

The percentage of error denotes the uniform dispersion of shading over the PV array. For the high percentage of error, the mismatch loss in the PV array is high and for the minimum percentage of error the mismatch loss will be low. The panel rating is given in Table.1

TABLE 1. Parameters of PV panel.

PARAMETERS	SPECIFICATION
Open circuit Voltage, VOC	10.8V
Short Circuit Current, ISC	1.25A
Maximum Voltage, Vm	9V
Maximum Current, Im	1.1A
Maximum Power, Pm	10Wp

A. PERFORMANCE ANALYSIS UNDER RANDOM SHADING CONDITION

Let consider the random shading pattern for the first case of analysis. The shading is not unique over the PV array. The shading pattern will not follow any kind of pattern like other shading condition. This kind of shading may occur in a random condition during the quick changing environmental conditions or the minor fault in the PV modules. The shading dispersion diagram and the P-V, I-V characteristic curves for the TCT, Sudoku, FPP, proposed array configuration and proposed array configuration after the reconfiguration is shown in Fig.6.

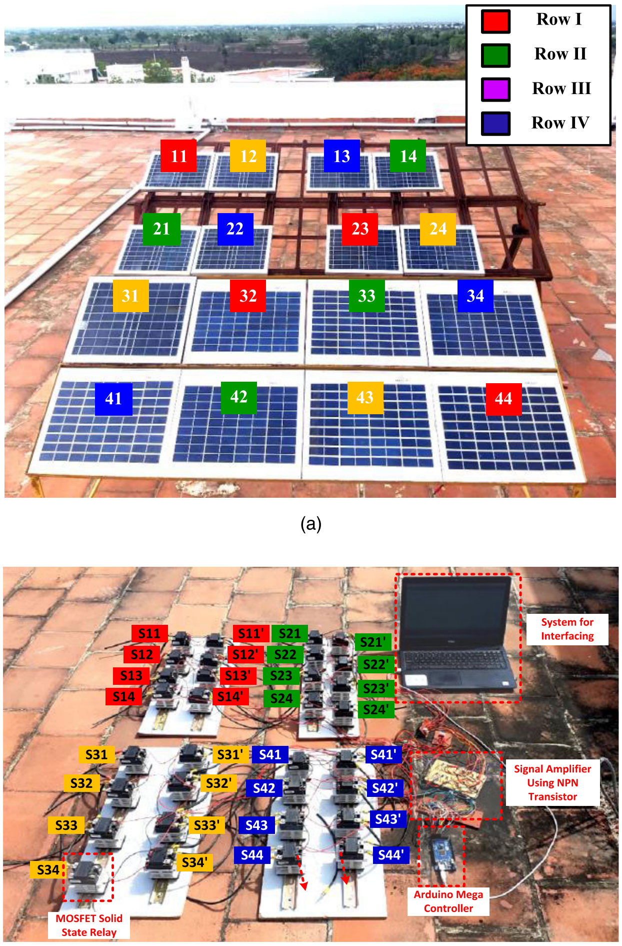

(a)

(b)

FIGURE 5. Structure of 4 × 4 PV array with proposed array configuration (b). Photograph of the hardware implementation of 4 × 4 switching matrix circuit.

In the first row the panel receives the irradiation as 400W/m2, 400W/m2, 200W/m2 and 800W/m2. The second row receives the irradiation as 800W/m2, 400W/m2, 600W/m2 and 800W/m2. Third row of the PV array receives 600W/m2, 950W/m2, 200W/m2 and 600W/m2 and the last row receives 800W/m2, 950W/m2, 950W/m2 and 400W/m2. The shading dispersion rate of the PV array can be found by analyzing the current generation of each row and by the percentage of error.

1) ANALYSIS OF ROW CURRENT GENERATION

The array configuration is made up of TCT connection. The current generation of each row can be calculated For the TCT configuration, Current generation of each row can be measured as,

$$\begin{aligned} I_{mR1} &= \left[\left(\frac{400}{1000}\times I_m\right)+\left(\frac{400}{1000}\times I_m\right)+\left(\frac{200}{1000}\times I_m\right)\right.\\ &\quad\left.+\left(\frac{800}{1000}\times I_m\right)\right]=1.8I_m\\ I_{mR2} &= \left[\left(\frac{800}{1000}\times I_m\right)+\left(\frac{400}{1000}\times I_m\right)+\left(\frac{600}{1000}\times I_m\right)\right.\\ &\quad\left.+\left(\frac{800}{1000}\times I_m\right)\right]=2.6I_m\\ I_{mR3} &= \left[\left(\frac{600}{1000}\times I_m\right)+\left(\frac{950}{1000}\times I_m\right)+\left(\frac{200}{1000}\times I_m\right)\right.\\ &\quad\left.+\left(\frac{600}{1000}\times I_m\right)\right]=2.35I_m\\ I_{mR4} &= \left[\left(\frac{800}{1000}\times I_m\right)+\left(\frac{950}{1000}\times I_m\right)+\left(\frac{950}{1000}\times I_m\right)\right.\\ &\quad\left.+\left(\frac{400}{1000}\times I_m\right)\right]=3.1I_m \end{aligned}$$

For the Sudoku puzzle pattern configuration, Current generation of each row can be measured as,

$$\begin{aligned} I_{mR1} &= \left[\left(\frac{400}{1000}\times I_m\right)+\left(\frac{400}{1000}\times I_m\right)+\left(\frac{200}{1000}\times I_m\right)\right.\\ &\quad\left.+\left(\frac{400}{1000}\times I_m\right)\right]=1.2I_m\\ I_{mR2} &= \left[\left(\frac{800}{1000}\times I_m\right)+\left(\frac{950}{1000}\times I_m\right)+\left(\frac{950}{1000}\times I_m\right)\right.\\ &\quad\left.+\left(\frac{800}{1000}\times I_m\right)\right]=3.5I_m\\ I_{mR3} &= \left[\left(\frac{400}{1000}\times I_m\right)+\left(\frac{950}{1000}\times I_m\right)+\left(\frac{200}{1000}\times I_m\right)\right.\\ &\quad\left.+\left(\frac{800}{1000}\times I_m\right)\right]=2.35I_m\\ I_{mR4} &= \left[\left(\frac{800}{1000}\times I_m\right)+\left(\frac{400}{1000}\times I_m\right)+\left(\frac{600}{1000}\times I_m\right)\right.\\ &\quad\left.+\left(\frac{600}{1000}\times I_m\right)\right]=2.4I_m \end{aligned}$$

The current generation of the Futoshiki Puzzle pattern can be measured as,

$$\begin{aligned} I_{mR1} &= \left[\left(\frac{400}{1000}\times I_m\right)+\left(\frac{950}{1000}\times I_m\right)+\left(\frac{950}{1000}\times I_m\right)\right.\\ &\quad\left.+\left(\frac{800}{1000}\times I_m\right)\right]=3.1I_m\\ I_{mR2} &= \left[\left(\frac{800}{1000}\times I_m\right)+\left(\frac{950}{1000}\times I_m\right)+\left(\frac{200}{1000}\times I_m\right)\right.\\ &\quad\left.+\left(\frac{800}{1000}\times I_m\right)\right]=3.25I_m\\ I_{mR3} &= \left[\left(\frac{800}{1000}\times I_m\right)+\left(\frac{400}{1000}\times I_m\right)+\left(\frac{600}{1000}\times I_m\right)\right.\\ &\quad\left.+\left(\frac{600}{1000}\times I_m\right)\right]=2.4I_m\\ I_{mR4} &= \left[\left(\frac{600}{1000}\times I_m\right)+\left(\frac{400}{1000}\times I_m\right)+\left(\frac{200}{1000}\times I_m\right)\right.\\ &\quad\left.+\left(\frac{400}{1000}\times I_m\right)\right]=1.6I_m \end{aligned}$$

The current generation of the proposed array configuration can be measured as,

$$\begin{aligned} I_{mR1} &= \left[\left(\frac{400}{1000}\times I_m\right)+\left(\frac{600}{1000}\times I_m\right)+\left(\frac{950}{1000}\times I_m\right)\right.\\ &\quad\left.+\left(\frac{400}{1000}\times I_m\right)\right]=2.35I_m\\ I_{mR2} &= \left[\left(\frac{800}{1000}\times I_m\right)+\left(\frac{200}{1000}\times I_m\right)+\left(\frac{950}{1000}\times I_m\right)\right.\\ &\quad\left.+\left(\frac{800}{1000}\times I_m\right)\right]=2.75I_m\\ I_{mR3} &= \left[\left(\frac{600}{1000}\times I_m\right)+\left(\frac{950}{1000}\times I_m\right)+\left(\frac{400}{1000}\times I_m\right)\right.\\ &\quad\left.+\left(\frac{800}{1000}\times I_m\right)\right]=2.75I_m\\ I_{mR4} &= \left[\left(\frac{800}{1000}\times I_m\right)+\left(\frac{200}{1000}\times I_m\right)+\left(\frac{400}{1000}\times I_m\right)\right.\\ &\quad\left.+\left(\frac{600}{1000}\times I_m\right)\right]=2I_m \end{aligned}$$

The current generation of the proposed method after the reconfiguration is measured in two steps. The current generation of the fixed part rows and the adaptive part rows have been measured separately. Based on the reconfiguration algorithm, the fixed part row is connected with the adaptive part row. Then the current generation of the entire row is calculated. The current generation of the flexible unit rows are measured as,

$$\begin{aligned} I_{mFR1} &= \left[\left(\frac{400}{1000}\times I_m\right)+\left(\frac{600}{1000}\times I_m\right)\right]=1I_m\\ I_{mFR2} &= \left[\left(\frac{800}{1000}\times I_m\right)+\left(\frac{200}{1000}\times I_m\right)\right]=1I_m\\ I_{mFR3} &= \left[\left(\frac{600}{1000}\times I_m\right)+\left(\frac{950}{1000}\times I_m\right)\right]=1.55I_m\\ I_{mFR4} &= \left[\left(\frac{800}{1000}\times I_m\right)+\left(\frac{200}{1000}\times I_m\right)\right]=1I_m \end{aligned}$$

The current generation of the adaptive unit rows are measured as,

$$\begin{aligned} I_{mSR1} &= \left[\left(\frac{950}{1000}\times I_m\right)+\left(\frac{400}{1000}\times I_m\right)\right]=1.35I_m\\ I_{mSR2} &= \left[\left(\frac{950}{1000}\times I_m\right)+\left(\frac{800}{1000}\times I_m\right)\right]=1.75I_m\\ I_{mSR3} &= \left[\left(\frac{400}{1000}\times I_m\right)+\left(\frac{800}{1000}\times I_m\right)\right]=1.2I_m\\ I_{mSR4} &= \left[\left(\frac{400}{1000}\times I_m\right)+\left(\frac{600}{1000}\times I_m\right)\right]=1I_m \end{aligned}$$

The reconfiguration algorithm connects the maximum power generating row of Flexible unit with the minimum

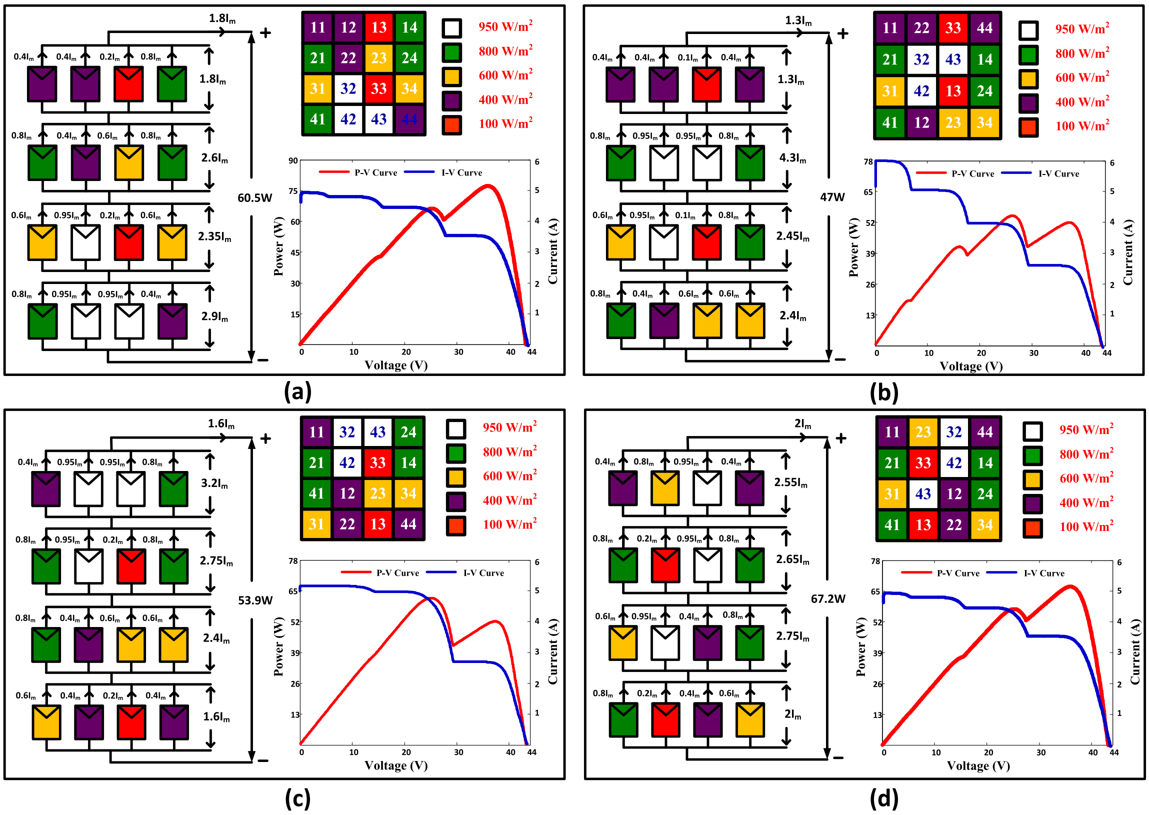

(a)

11	12	13	14
21	22	23	24
31	32	33	34
41	42	43	44

(b)

11	22	33	44
21	32	43	14
31	42	13	24
41	12	23	34

(c)

11	32	43	24
21	42	33	14
41	12	23	34
31	22	13	44

(d)

11	23	32	44
21	33	42	14
31	43	12	24
41	13	22	34

FIGURE 6. **Current flow diagram with shade dispersion matrix and P-V, I-V characteristics for (a) TCT (b) Sudoku (c) Futoshiki (d) proposed array configuration.**

power generation row of adaptive unit for executing the reconfiguration as shown in the Fig.9. The current generation of each row after the reconfiguration can be measured as,

$$\begin{aligned} I_{mR1} &= [I_{mFR3} + I_{mSR4}] = 2.55I_m \\ I_{mR2} &= [I_{mFR1} + I_{mSR3}] = 2.2I_m \\ I_{mR3} &= [I_{mFR2} + I_{mSR1}] = 2.35I_m \\ I_{mR4} &= [I_{mFR4} + I_{mSR2}] = 2.75I_m \end{aligned}$$

From equation (7), the percentage of error is calculated for analyzing the effectiveness of each configuration under the random shading condition. The purpose of the proposed array configuration is to uniformly disperse the shading effect to make each row with nearly even current generation. The percentage of error shows the uniformity of shade dispersion. The performance analysis is given in Table.2.

The TCT configuration has the error rate of 57.9% which has the rank of the third position. The percentage of error of the proposed configuration is 15.7% and after reconfiguration is 12% which lowers than all other configurations where the FPP configuration has the 44.3% of error rate which is higher in this random shading pattern. The random shading pattern may occur on any part of the PV array but the proposed method could distribute the effect of shading evenly in the PV array. The power output of the proposed configuration will be higher than other configuration because of the low percentage of error. The power generation and the shade dispersion matrix of the TCT, Sudoku, Futoshiki Configurations has shown in Fig.8. The High current generating row in the fixed part has been connected with the low current generating row of the adaptive part. The P-V and I-V characteristic curves of the reconfigured PV array has shown in Fig.8. The characteristic curve of all configurations has the multiple peaks i.e., many local maximum power points but the proposed configuration curve has nearly a smooth curve. It is also inferred that the proposed configuration has the global maximum power point as compared with other configurations.

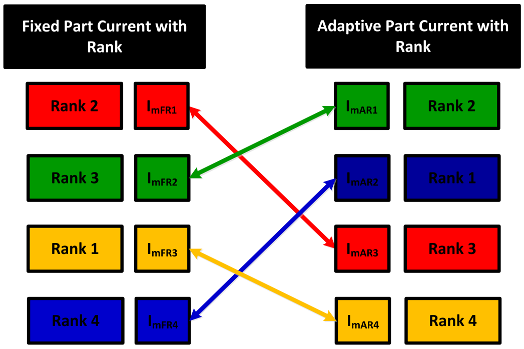

FIGURE 7. **Reconfiguration pattern establishment diagram.**

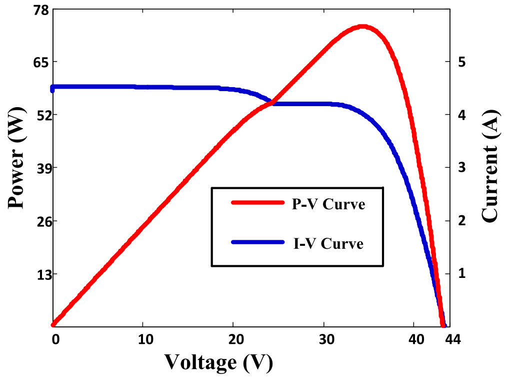

FIGURE 8. P-V and I-V characteristics after reconfiguration.

The power loss analysis is carried out to find the amount of power enhanced during the shading pattern. The short circuit current, open-circuit voltage, and the maximum power for all configurations have been derived from the Simulink output. Table.2 shows the power output and the power loss for each array configuration. The power loss can be calculated by using the following equation (8),

$$Power\_Loss = \left(\frac{P_{STC} - P_{OUT}}{P_{STC}}\right) \times 100 \tag{8}$$

B. PERFORMANCE ANALYSIS UNDER UNEVEN COLUMN SHADING CONDITION

The rows in the PV array are availed with irregular irradiation in the type of uneven column shading. The nearby objects are the main cautions for this kind of shading pattern. In this kind of shading pattern, TCT array configuration has very low power generation due to the shading in a single row. The shading pattern and the shade dispersion diagram of the all-array configuration under this shading pattern is shown in Fig.9.

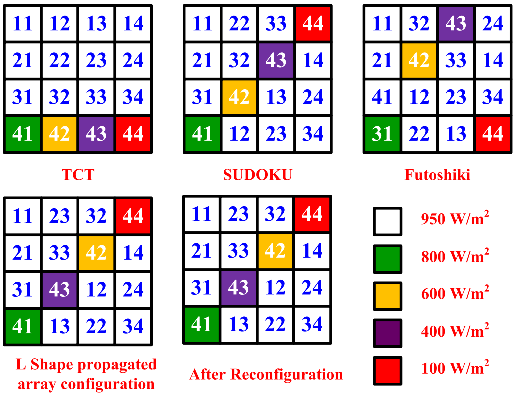

11	12	13	14
21	22	23	24
31	32	33	34
41	42	43	44

TCT

11	22	33	44
21	32	43	14
31	42	13	24
41	12	23	34

SUDOKU

11	32	43	24
21	42	33	14
41	12	23	34
31	22	13	44

Futoshiki

11	23	32	44
21	33	42	14
31	43	12	24
41	13	22	34

L Shape propagated array configuration

11	23	32	44
21	33	42	14
31	43	12	24
41	13	22	34

After Reconfiguration

⬜ 950 W/m^2
🟩 800 W/m^2
🟨 600 W/m^2
🟪 400 W/m^2
🟥 100 W/m^2

FIGURE 9. Matrix dispersion diagram under UC shading.

The first PV module in each row has affected by the shading that causes uneven shading pattern. The TCT is highly losing its performance in this shading whereas the other configurations disperse the shading evenly over the PV array that observed from the matrix dispersion diagram. The percentage of error is given in Table.2.

C. PERFORMANCE ANALYSIS UNDER UNEVEN ROW SHADING CONDITION

The UR shading occurs in the PV array that causes the uneven irradiance in each row of the PV array. This generally occurs due to the nearby objects or the environmental changes. The TCT configuration could withstand this kind of shading. The matrix dispersion diagram under UR shading pattern is shown in Fig.10.

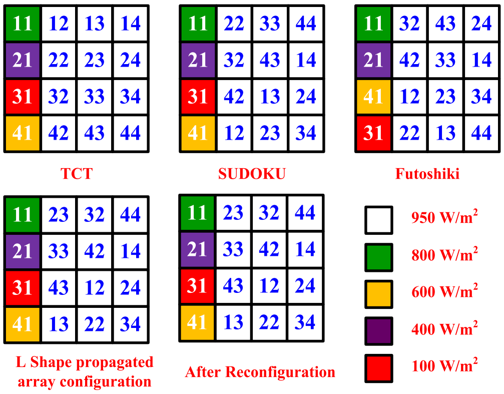

11	12	13	14
21	22	23	24
31	32	33	34
41	42	43	44

TCT

11	22	33	44
21	32	43	14
31	42	13	24
41	12	23	34

SUDOKU

11	32	43	24
21	42	33	14
41	12	23	34
31	22	13	44

Futoshiki

11	23	32	44
21	33	42	14
31	43	12	24
41	13	22	34

L Shape propagated array configuration

11	23	32	44
21	33	42	14
31	43	12	24
41	13	22	34

After Reconfiguration

⬜ 950 W/m^2
🟩 800 W/m^2
🟨 600 W/m^2
🟪 400 W/m^2
🟥 100 W/m^2

FIGURE 10. Matrix dispersion diagram under uneven row shading.

All configurations have an equal shade dispersion rate that also reflects in the percentage of error. Generally, this kind of shading does not cause more power loss in TCT but in Series parallel configuration this causes severe power loss. The percentage of error under UR shading is given in Table.2 All array configurations have an equal percentage of error that shows that all configurations had equally dispersed the shading over the PV array

D. PERFORMANCE ANALYSIS UNDER DIAGONAL SHADING CONDITION

In diagonal shading pattern, the PV modules in the diagonal position of the square or rectangular PV array has experiencing the shading due to the nearby taller narrow objects like towers, chimneys or by the clouds. The PV modules in the diagonal positions like P11, P22, P33, and P44 have received the irregular irradiation such as 800W/m2, 200W/m2, 400W/m2 and 800W/m2 whereas another PV module receives the irradiation as 950W/m2. The shading dispersion diagram of each array configuration is shown in Fig.11. The Sudoku configuration failed to disperse the shading evenly over the PV array. The shading is not completely dispersed in the Futoshiki and proposed array configuration which reflects the limitation of the static array configuration. This limitation of the static configuration has overcome by the proposed dynamic reconfiguration algorithm. The proposed configuration after reconfiguration shows the ability to overcome the limitation and disperse the shading as much as possible over the PV array.

TABLE 2. Performance comparison under various shading conditions.

SHADING TYPE	ARRAY CONFIGURATIONS	ImR1	ImR2	ImR3	ImR4	% OF ERROR	Im (A)	Pm (W)	POWER LOSS
Random	TCT	1.8Im	2.6Im	2.35m	3.1Im	57.9%	1.8	60.5	49.9%
	Sudoku	1.4Im	3.5Im	2.55Im	2.4Im	38.1%	1.4	47.0	60.0%
	FPP	3.1Im	2.75Im	2.4Im	1.6Im	44.4%	1.6	53.9	55.2%
	L-Shape	2.35Im	2.75Im	2.75Im	2Im	15.7%	2.1	67.2	44.0%
	AR	2.55Im	2.2Im	2.35Im	2.75Im	12.0%	2.3	73.9	38.4%
Uneven Column	TCT	3.8Im	3.8Im	3.8Im	2Im	47.4%	2	67.2	44.0%
	Sudoku	3.05Im	3.25Im	3.45Im	3.65Im	16.4%	3.05	102.5	14.6%
	FPP	3.25Im	3.45Im	3.65Im	3.05Im	16.4%	3.05	102.5	14.6%
	L-Shape	3.05Im	3.45Im	3.25Im	3.65Im	16.4%	3.05	102.5	14.6%
	AR	3.05Im	3.45Im	3.65Im	3.25Im	16.4%	3.05	102.5	14.6%
Uneven Row	TCT	3.65Im	3.25Im	3.05Im	3.45Im	16.4%	3.05	102.5	14.6%
	Sudoku	3.65Im	3.25Im	3.05Im	3.45Im	16.4%	3.05	102.5	14.6%
	FPP	3.65Im	3.25Im	3.05Im	3.45Im	16.4%	3.05	102.5	14.6%
	L-Shape	3.65Im	3.25Im	3.05Im	3.45Im	16.4%	3.05	102.5	14.6%
	AR	3.65Im	3.45Im	3.25Im	3.05Im	16.4%	3.05	102.5	14.6%
Diagonal	TCT	3.65Im	3.05Im	3.25Im	3.65Im	16.4%	3.05	102.5	14.6%
	Sudoku	2.2Im	3.8Im	3.8Im	3.8Im	42.1%	2.2	73.9	42.1%
	FPP	3.65Im	3.25Im	3.8Im	2.9Im	23.7%	2.9	97.4	23.7%
	L-Shape	3.5Im	3.25Im	3.8Im	2.9Im	19.7%	3.05	102.5	19.7%
	AR	3.05Im	3.65Im	3.65Im	3.25Im	16.4%	3.05	102.5	16.4%
Short & Narrow	TCT	3.3Im	2.5Im	3.8Im	3.8Im	32.4%	2.5	84.0	45%
	Sudoku	2.9Im	3.25Im	3.8Im	3.45Im	23.7%	2.9	97.4	49%
	FPP	3.65Im	3.25Im	3.45Im	3.05Im	16.4%	3.1	102.5	14.6%
	L-Shape	3.65Im	3.25Im	3.45Im	3.05Im	16.4%	3.1	102.5	14.6%
	AR	3.05Im	3.45Im	3.65Im	3.25Im	16.4%	3.1	102.5	14.6%
Short & Wide	TCT	1.95Im	2.75Im	2.35Im	3.8Im	48.7%	1.96	65.5	45.4%
	Sudoku	1.75Im	3.3Im	2.5Im	3.3Im	47.0%	1.75	58.8	51.0%
	FPP	2.9Im	2.7Im	3.3Im	1.95Im	40.9%	1.95	65.5	45.4%
	L-Shape	2.75Im	2.7Im	2.9Im	2.5Im	13.8%	2.5	84.0	30.0%
	AR	2.7Im	2.7Im	2.75Im	2.7Im	1.8%	2.7	90.7	24.4%
Long & Narrow	TCT	1.8Im	2.4Im	3.8Im	3.8Im	52.6%	1.8	60.5	49.6%
	Sudoku	2.9Im	3.1Im	2.3Im	3.5Im	34.3%	2.3	77.3	35.6%
	FPP	2.5Im	3.1Im	3.5Im	2.7Im	28.6%	2.5	84.0	30.0%
	L-Shape	3.1Im	3.1Im	2.9Im	2.7Im	12.9%	2.7	90.7	24.4%
	AR	2.9Im	3.1Im	2.75Im	3.05Im	11.3%	2.75	92.4	23.0%
Long & Wide	TCT	1.6Im	2Im	2m	3.8Im	57.9%	1.6	53.8	55.2%
	Sudoku	2.15Im	2.15Im	1.95Im	3.15Im	38.1%	1.95	65.5	45.4%
	FPP	2.15Im	2.35Im	3.15Im	1.75Im	44.4%	1.75	58.8	51.0%
	L-Shape	2.55Im	2.35Im	2.15Im	2.35Im	15.7%	2.15	72.2	39.8%
	AR	2.35Im	2.2Im	2.35Im	2.5Im	12.0%	2.2	73.9	38.4%

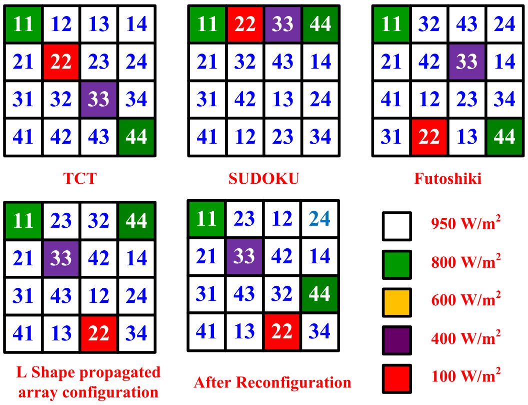

FIGURE 11. Matrix dispersion diagram under diagonal shading.

The efficiency of the proposed array configuration is given in Table.2 with the percentage of error. The Futoshiki and Sudoku pattern has the highest percentage of error as compared to others. The proposed array configuration is also had a high percentage of error but this can be further reduced by the reconfiguration. The characteristic curve of all configurations under the diagonal shading is shown in Fig.12. Whereas the TCT and the configuration after the reconfiguration have a similar P-V and I-V curves. The Futoshiki and Sudoku patterns had the uneven shade dispersion over the PV array that reflects in the P-V curve as the multiple peaks. Whereas the proposed array configuration had less number of peaks that shows the power enhancement over the existing configurations.

E. PERFORMANCE ANALYSIS UNDER SHORT & NARROW SHADING CONDITION

The short and narrow shading may occur in the PV array due to the nearby objects that covers 25% of PV array size. The P11, P12, P13, and P22 have experienced the shading in S&N. Shading dispersion diagram and the shading pattern under the short and narrow is shown in Fig.13.

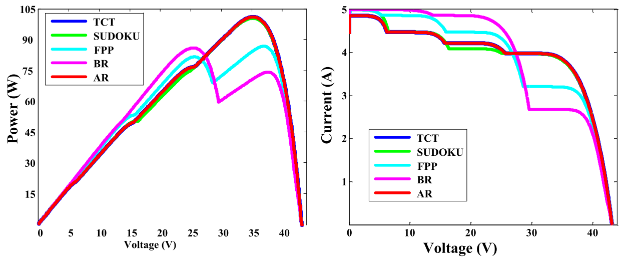

FIGURE 12. P-V and I-V characteristics under diagonal shading.

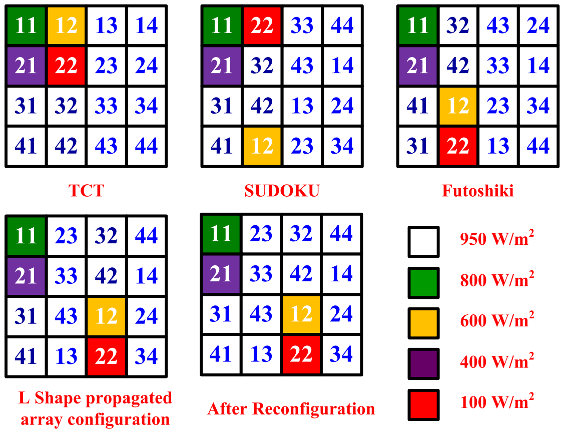

FIGURE 13. Matrix dispersion diagram under short and Narrow.

It is inferred that the shading has uniformly dispersed in the Futoshiki configuration. The power output by the Futoshiki configuration, proposed configuration and after reconfiguration is the same due to the third and fourth column has an equal irradiation level. The percentage of error under the short and narrow shading condition has given in Table.2.

The TCT and Sudoku pattern has a high-level percentage of error in this shading pattern. The P-V and I-V characteristics of all configurations under the short and narrow shading pattern are shown in Fig.14. The characteristic curve of TCT and Sudoku configurations has multiple peaks due to the uneven shade dispersion. The Futoshiki and the proposed configurations had the less no of peaks and also had the maximum power points as compared to the existing configurations.

F. PERFORMANCE ANALYSIS UNDER SHORT & WIDE SHADING CONDITION

The shading dispersion under the short and wide shading pattern is discussed in this section. This kind of shading affects 75% of the PV area. The shade dispersion is much required for this shading condition due to the high power loss. The shade dispersion can enhance more power in this kind of shading but it depends on the uniformity. The proposed reconfiguration method uniformly disperses the shading over the PV array. The matrix diagram of the shade dispersion is shown in Fig.15.

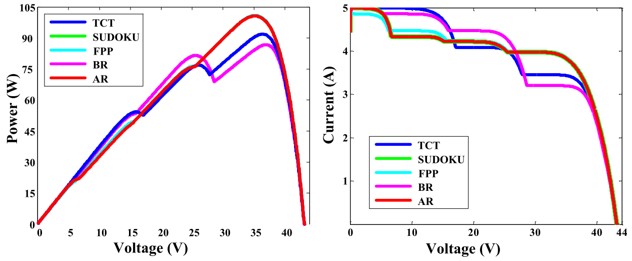

FIGURE 14. P-V and I-V characteristics under S&N shading.

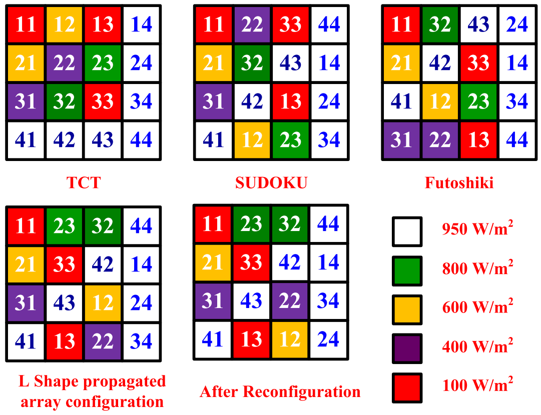

FIGURE 15. Matrix dispersion diagram under short and wide.

The percentage of error compared in Table.2. TCT configuration is not efficient in highly shaded PV array that also reflects in the percentage of error. The proposed reconfiguration allows the PV array to disperse the shading uniformly even under the high shading condition like short and wide. The Futoshiki and Sudoku configuration has a high percentage of error that was minimized in the proposed configuration.

The P-V and I-V characteristics of all configurations under the short and wide shading pattern are shown in Fig.16. The red colour curve shows the characteristics of the proposed reconfiguration method which has one small peak in the centre where the Futoshiki, Sudoku and the TCT pattern has multiple peaks in the P-V curve. It is inferred that the proposed reconfiguration method can produce the minimum number of peaks in the characteristic curve with maximum power generation.

G. PERFORMANCE ANALYSIS UNDER LONG AND NARROW SHADING CONDITION

The long and narrow shading affects the irradiance of PV array around 50% which reduced half of the power generation in TCT configuration. The proposed reconfiguration algorithm is more effective for this kind of shading pattern. At first, the proposed reconfiguration disperses the shading as much as possible later the reconfiguration algorithm disperse the effect of shading evenly over the PV array. The matrix dispersion diagram of shading is shown in Fig.17. The Futoshiki

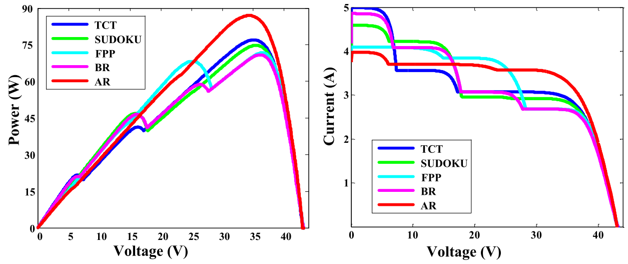

FIGURE 16. P-V and I-V characteristics under S&W shading.

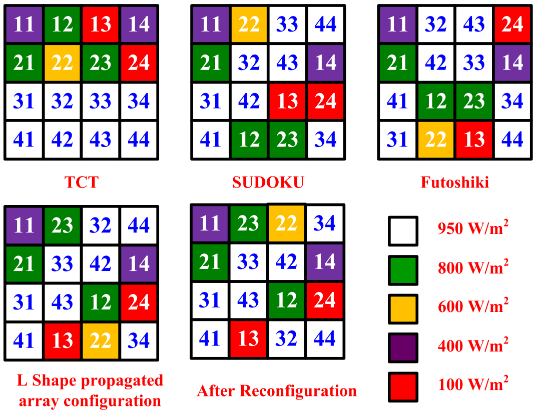
11 12 13 14
21 22 23 24
31 32 33 34
41 42 43 44
TCT
11 22 33 44
21 32 43 14
31 42 13 24
41 12 23 34
SUDOKU
11 32 43 24
21 42 33 14
41 12 23 34
31 22 13 44
Futoshiki
11 23 32 44
21 33 42 14
31 43 12 24
41 13 22 34
L Shape propagated array configuration
11 23 22 34
21 33 42 14
31 43 12 24
41 13 32 44
After Reconfiguration
950 W/m²
800 W/m²
600 W/m²
400 W/m²
100 W/m²

FIGURE 17. Matrix dispersion diagram under long and Narrow.

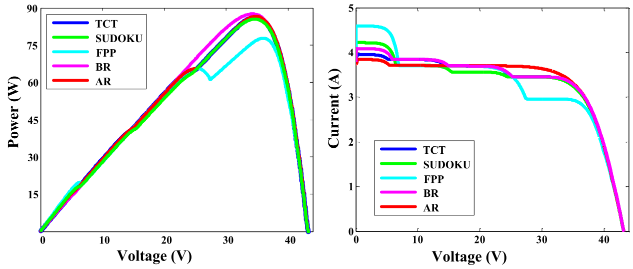

FIGURE 18. P-V and I-V characteristics under L&N shading.

and Sudoku configuration has a high percentage of error where the proposed configuration minimized the percentage of error more than half of the existing. It shows the ability of the proposed configuration to disperse the shading evenly in all rows.

The P-V and I-V characteristic curves under the L&N shading pattern have shown in Fig.18. The Sudoku, TCT, and Futoshiki configurations had the more no of peaks in the characteristic curves. The proposed configuration has the one up and down in the characteristic curve that closes to the smooth curve. The characteristic curves of the PV system before and after reconfiguration nearly close to each other.

H. PERFORMANCE ANALYSIS UNDER LONG AND WIDE SHADING CONDITION

The long and wide shading pattern affects around 75% to 80% of irradiation of the PV array. This kind of shading is mostly possible by the clouds, by the unavoidable objects and by the temporary constructions. The PV array requires the uniform shade dispersion to minimize the mismatch losses. In this proposed method the PV can disperse the shading based on the power generation. It makes the even power generating row so that the maximum power can be extracted as much as possible. The matrix dispersion diagram of the array configurations under the L&W shading pattern is shown in Fig.18. The TCT, Sudoku and FPP configurations have a high percentage of error in the L&W shading pattern. That also reduces power output. The proposed configuration has less than 10% of error that allows the rows in PV array to generate nearly equal current with each other. The Power output the amount of power loss in each array configuration has given in Table.2.

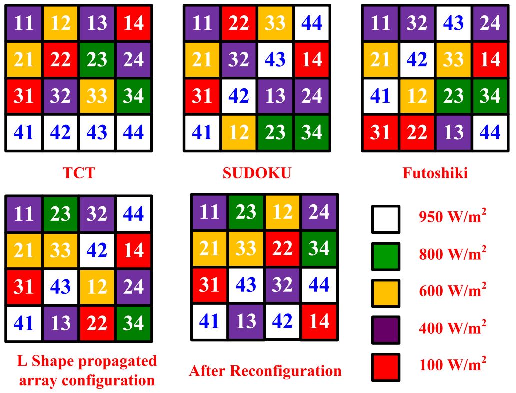
11 12 13 14
21 22 23 24
31 32 33 34
41 42 43 44
TCT
11 22 33 44
21 32 43 14
31 42 13 24
41 12 23 34
SUDOKU
11 32 43 24
21 42 33 14
41 12 23 34
31 22 13 44
Futoshiki
11 23 32 44
21 33 42 14
31 43 12 24
41 13 22 34
L Shape propagated array configuration
11 23 12 24
21 33 22 34
31 43 32 44
41 13 42 14
After Reconfiguration
950 W/m²
800 W/m²
600 W/m²
400 W/m²
100 W/m²

FIGURE 19. Matrix dispersion diagram under long and wide.

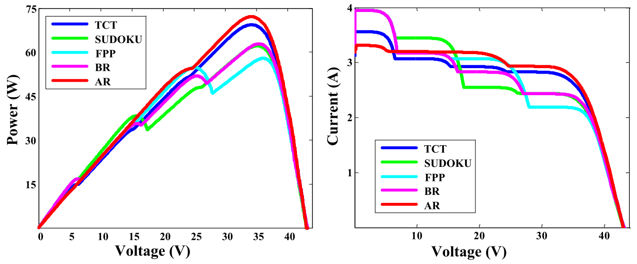

FIGURE 20. P-V and I-V characteristics under L&W shading.

The P-V and I-V characteristics of the PV array configurations in L&W shading pattern is shown in Fig.20. It is inferred that the proposed method after reconfiguration has a smooth P-V and I-V curve whereas all other configurations have the curve with multiple peaks. This difference shows the effectiveness of the proposed method for power enhancement under the various shading conditions.

I. OUTPUT ANALYSIS

The maximum current and the power output of the 4 × 4 PV array is measured by the Arduino controller, current sensor and the potential divider. Based on the measured values the P-V and I-V characteristic curves were plotted and the power output comparison were discussed in the result and discussion

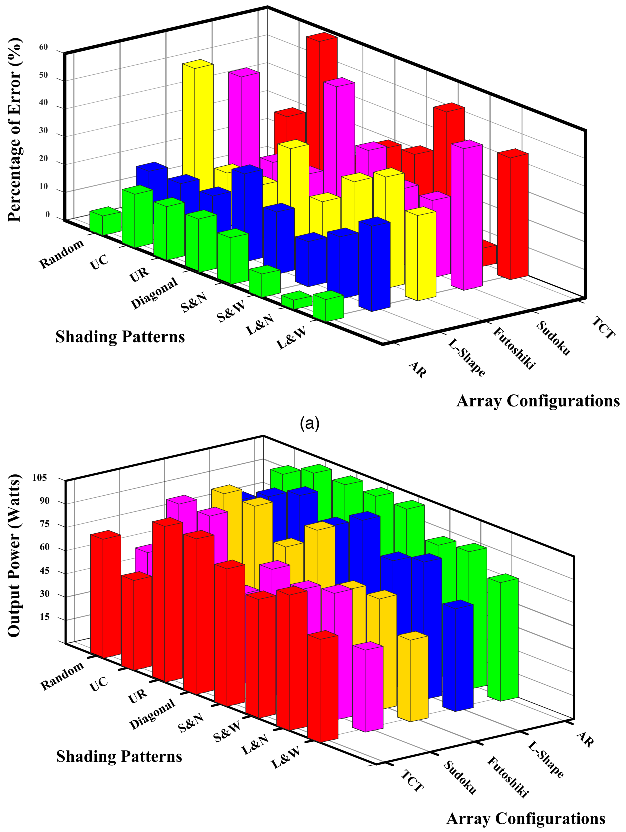

(a)

(b)

FIGURE 21. Percentage of error comparison chart (b) Output power comparison chart.

section. It is observed that the proposed configuration has the consi1stency of shade dispersion in all kind of shading pattern, whereas the other configuration is good in some specific shading pattern and failed to perform in others. The Futoshiki and the Sudoku configurations have the good power generation near to the proposed method in UCS, URS, SN, Diagonal shading patterns. But the proposed array configuration and reconfiguration algorithm has dispersed the maximum level of shading in all cases of shading pattern. The proposed method has the unique performance in all kind of shading patterns. The percentage of error and the power output shows the effectiveness of the proposed configuration over the other array configurations and it has plotted as the bar chart shown in Fig.21(a) and Fig.21. (b).

IV. CONCLUSION

The five types of array configurations including the proposed method have been analyzed with the eight kinds of possible shading patterns. The shading patterns like UR, UC, and Diagonal were considered as the minor shadings that do not highly affects the power output. In these shadings, the existing configurations such as TCT, Sudoku and the FPP could disperse the shading uniformly over the PV array whereas the proposed method disperses too. While considering the major shading patterns like random, S&N, S&W, L&N and L&W the existing array configurations failed to disperse the shading evenly. The percentage of error under the major shading patterns is more than 35% in the existing configurations where the proposed configuration had less than 20% for the all-kind shading patterns. It is inferred that the existing configurations are good in the minor shading patterns but failed to perform under the major shading patterns. The proposed L-shape array configuration performs better than the all-other array configurations. The performance of the L-shape configuration is further enhanced by the proposed reconfiguration scheme. Shading level and its pattern are not a constraint for the proposed method because it makes the even current generating rows by reconfigure the PV modules. The implementation of the proposed L-Shape propagated array configuration is very simple as like the existing array configurations and it can be implemented on any sized PV systems. This method will be commercial solution to the PV system for overcoming the mismatch losses. The initial cost is higher than the existing configurations (not much higher); however, the payback period is very low from the power generation of the PV array.

NOMENCLATURE

ACO	Ant Colony Optimization
ANN	Artificial Neural Network
BL	Bridge Linked
FPP	Futoshiki Puzzle Pattern
GMPP	Global Maximum Power Point
HC	Honey Comb
I_m	Maximum current
I_{mFRi}	Row current generation of fixed unit
I_{mRi}	Maximum current output of PV Row
I_{mSRi}	Row current generation of static unit
InC	Incremental Conductance
I_{out}	Current Output
I_{SC}	Short Circuit Current
I_{SCFURi}	Short Circuit Current of Flexible Units
$I_{SCFURsort}$	Sorted Short Circuit Current of Flexible Units
I_{SCRi}	Short Circuit Current of Row
I_{SCRmax}	Maximum Short Circuit Current of Row
I_{SCRmin}	Minimum Short Circuit Current of Row
I_{SCSURi}	Short Circuit Current of Static Units
$I_{SCSURsort}$	Sorted Short Circuit Current of Static Units
LMPP	Local Maximum Power Point
MPP	Maximum Power Point
MPPT	Maximum Power Point Tracking
P&O	Perturb and observe
P_m	Maximum Power Output
PSO	Particle Swarm Optimization
Se-P	Series Parallel
TCT	Total Cross Tied
V_m	Maximum Voltage
V_{OC}	Open Circuit Voltage

REFERENCES

[1] M. Premkumar, U. Subramaniam, T. S. Babu, R. M. Elavarasan, and L. Mihet-Popa, "Evaluation of mathematical model to characterize the performance of conventional and hybrid PV array topologies under static and dynamic shading patterns," *Energies*, vol. 13, no. 12, p. 3216, Jun. 2020.

[2] S. K. Kar, A. Sharma, and B. Roy, "Solar energy market developments in india," *Renew. Sustain. Energy Rev.*, vol. 62, pp. 121–133, Sep. 2016, doi: 10.1016/j.rser.2016.04.043.

[3] K. Konnerth, "Junction heating in GaAs injection lasers," *Proc. IEEE*, vol. 53, no. 4, pp. 397–398, 1965.

[4] D. Yousri, T. S. Babu, E. Beshr, M. B. Eteiba, and D. Allam, "A robust strategy based on marine predators algorithm for large scale photovoltaic array reconfiguration to mitigate the partial shading effect on the performance of PV system," *IEEE Access*, vol. 8, pp. 112407–112426, 2020.

[5] M. A. A. Mamun, M. Hasanuzzaman, and J. Selvaraj, "Experimental investigation of the effect of partial shading on photovoltaic performance," *IET Renew. Power Gener.*, vol. 11, no. 7, pp. 912–921, Jun. 2017, doi: 10.1049/iet-rpg.2016.0902.

[6] P. R. Satpathy and R. Sharma, "Reliability and losses investigation of photovoltaic power generators during partial shading," *Energy Convers. Manage.*, vol. 223, Nov. 2020, Art. no. 113480.

[7] V. Gupta, M. Sharma, R. K. Pachauri, and K. N. D. Babu, "Comprehensive review on effect of dust on solar photovoltaic system and mitigation techniques," *Sol. Energy*, vol. 191, pp. 596–622, Oct. 2019.

[8] P. Guerriero, P. Tricoli, and S. Daliento, "A bypass circuit for avoiding the hot spot in PV modules," *Sol. Energy*, vol. 181, pp. 430–438, Mar. 2019, doi: 10.1016/j.solener.2019.02.010.

[9] S. K. Kollimalla and M. K. Mishra, "Variable perturbation size adaptive P&O MPPT algorithm for sudden changes in irradiance," *IEEE Trans. Sustain. Energy*, vol. 5, no. 3, pp. 718–728, Jul. 2014, doi: 10.1109/TSTE.2014.2300162.

[10] K. Jain, M. Gupta, and A. Kumar Bohre, "Implementation and comparative analysis of P&O and INC MPPT method for PV system," in *Proc. 8th IEEE India Int. Conf. Power Electron. (IICPE)*, Dec. 2018, pp. 1–6.

[11] A. Muhammad, T. S. Babu, V. K. Ramachandaramurthy, D. Yousri, and J. B. Ekanayake, "Static and dynamic reconfiguration approaches for mitigation of partial shading influence in photovoltaic arrays," *Sustain. Energy Technol. Assessments* vol. 40, Apr. 2020, Art. no. 100738.

[12] D. Yousri, T. S. Babu, D. Allam, V. K. Ramachandaramurthy, E. Beshr, and M. B. Eteiba, "Fractional chaos maps with flower pollination algorithm for partial shading mitigation of photovoltaic systems," *Energies*, vol. 12, no. 18, p. 3548, Sep. 2019.

[13] S. R. Pendem and S. Mikkili, "Modeling, simulation and performance analysis of solar PV array configurations (Series, Series–Parallel and Honey-Comb) to extract maximum power under Partial Shading Conditions," *Energy Rep.*, vol. 4, pp. 274–287, Nov. 2018, doi: 10.1016/j.egyr.2018.03.003.

[14] T. Wongwuttanasatian, "Effect of partial shading patterns and degrees of shading on Total Cross-Tied (TCT) photovoltaic array configuration," *Energy Procedia*, vol. 153, pp. 35–41, Oct. 2018, doi: 10.1016/j.egypro.2018.10.028.

[15] D. Yousri, T. S. Babu, S. Mirjalili, N. Rajasekar, and M. A. Elaziz, "A novel objective function with artificial ecosystem-based optimization for relieving the mismatching power loss of large-scale photovoltaic array," *Energy Convers. Manage.*, vol. 225, Dec. 2020, Art. no. 113385.

[16] S. C. Christabel, A. Srinivasan, and D. P. Winston, "Couple matching best generation algorithm for partially shaded photovoltaic systems," *J. Electr. Eng*, vol. 16, pp. 328–391, Sep. 2016.

[17] D. Yousri, S. B. Thanikanti, K. Balasubramanian, A. Osama, and A. Fathy, "Multi-objective grey wolf optimizer for optimal design of switching matrix for shaded PV array dynamic reconfiguration," *IEEE Access*, vol. 8, no. 2020, pp. 159931–159946.

[18] T. S. Babu, D. Yousri, and K. Balasubramanian, "Photovoltaic array reconfiguration system for maximizing the harvested power using population-based algorithms," *IEEE Access*, vol. 8, pp. 109608–109624, 2020.

[19] D. Prince Winston, S. Kumaravel, B. Praveen Kumar, and S. Devakirubakaran, "Performance improvement of solar PV array topologies during various partial shading conditions," *Sol. Energy*, vol. 196, pp. 228–242, Jan. 2020, doi: 10.1016/j.solener.2019.12.007.

[20] A. Srinivasan, S. Devakirubakaran, and S. B. Meenakshi, "Mitigation of mismatch losses in solar PV system—Two-step reconfiguration approach," *Sol. Energy*, vol. 206, pp. 640–654, Aug. 2020, doi: 10.1016/j.solener.2020.06.004.

A. SRINIVASAN (Member, IEEE) received the B.E. degree in electrical and electronics engineering from Manonmaniam Sundaranar University, Tirunelveli, in 1995, and the M.E. degree in power systems engineering and the Ph.D. degree from Anna University, Chennai, in 2004 and 2014, respectively. He has more than 18 years of experience in teaching to both postgraduate and undergraduate students. He is currently a Professor and the Head of the Department of Electrical and Electronics Engineering, Sethu Institute of Technology. He has published one text book titled *Electrical Power Systems: Analysis, Security and Deregulation* (PHI, Delhi). He has published/presented 25 articles in international/national journals and conferences. His main research interests include power system restructuring and solar energy. He was a recipient of project grants from the Department of Science and Technology (DST), Solar Energy Research Initiative (SERI) Schemes.

S. DEVAKIRUBAKARAN received the B.E. degree in electrical and electronics engineering and the M.E. degree in power systems engineering from Anna University, Chennai, in 2014 and 2016, respectively. He is currently a Junior Research Fellow (JRF) with the Department of Electrical and Electronics Engineering, Sethu Institute of Technology. He is also doing the research at the Department of Science and Technology (DST), Solar Energy Research Initiative (SERI) Scheme Project. His main research interests include power systems, renewable energy systems, and solar photovoltaic systems.

B. MEENAKSHI SUNDARAM received the B.E. degree in electrical and electronics engineering from Madurai Kamaraj University, Madurai, in 1993, and the M.E. degree in power electronics and drives and the Ph.D. degree from Anna University, Chennai, in 2004 and 2018, respectively. He has more than 20 years of teaching experience. He is currently an Associate Professor with the Department of Electrical and Electronics Engineering, Sethu Institute of Technology. He is also the Co-Principal Investigator of the research project grants from the Department of Science and Technology (DST), Solar Energy Research Initiative (SERI) Schemes. He has published one textbook titled *Power Electronics*. He has published/presented 15 papers in international/national journals and conferences. His main research interests include power electronics for renewable energy and electrical drives.

PRAVEEN KUMAR BALACHANDRAN received the B.E. degree in electrical and electronics engineering and the M.E. and Ph.D. degrees in power systems engineering from Anna University, Chennai, India, in 2014, 2016, and 2019, respectively. He is currently working as an Assistant Professor with the Department of Electrical and Electronics Engineering (EEE), Bharat Institute of Engineering and Technology, Hyderabad, India. His current research interests include solar photovoltaics, and solar still and renewable energy systems.

SANTHAN KUMAR CHERUKURI received the B.Tech. degree in electrical and electronics engineering from JNTUK, Kakinada, India, in 2009, the M.Tech degree in power systems engineering from Acharya Nagarjuna University, Guntur, India, in 2012, and the Ph.D. degree in electrical and electronics engineering from JNTUK, in 2019. He is currently working as an Associate Professor and the Head of the Department, Department of Electrical and Electronics Engineering, Lords Institute of Engineering and Technology, Hyderabad, India. His current research interests include Solar PV Systems, PV Reconfiguration, Optimization of Power Systems, and Hybrid Energy Systems.

D. PRINCE WINSTON (Member, IEEE) received the B.E. degree in electrical and electronics engineering, the M.E. degree in power electronics and drives, and the Ph.D. degree from Anna University, Chennai, India, in 2006, 2008, and 2013, respectively. He is currently working as a Professor with the Department of Electrical and Electronics Engineering, Kamaraj College of Engineering and Technology, Madurai, India. He has published 35 research articles in several reputed international journals. His current research interests include solar PV, solar still, energy conservation in electric motor drives, power converters, power quality, and electric vehicles.

THANIKANTI SUDHAKAR BABU (Senior Member, IEEE) received the B.Tech. degree from Jawaharlal Nehru Technological University at Ananthapur, Ananthapur, India, in 2009, the M.Tech. degree in power electronics and industrial drives from Anna University, Chennai, India, in 2011, and the Ph.D. degree from VIT University, Vellore, India, in 2017.

From 2019 to 2020, he was associated with the Institute of Power Engineering, Universiti Tenaga Nasional (UNITEN), Malaysia, as a Postdoctoral Researcher. He is currently working as an Associate Professor with the Department of Electrical Engineering, Chaitanya Bharathi Institute of Technology, Hyderabad, India. He has published more than 60 research articles in various renowned international journals. His research interests include the design and implementation of solar PV systems, renewable energy resources, power management for hybrid energy systems, storage systems, fuel cell technologies, electric vehicles, and smart grids. He has been acting as an Editorial Board Member and a Reviewer of various reputed journals, such as the IEEE and IEEE ACCESS, IET, Elsevier, and Taylor and Francis.

HASSAN HAES ALHELOU (Senior Member, IEEE) is currently a Faculty Member with Tishreen University, Lattakia, Syria. He is also with University College Dublin, Ireland. He has published more than 130 research articles in the high-quality peer-reviewed journals and international conferences. He has participated in more than 15 industrial projects. His major research interests include power systems, power system dynamics, power system operation and control, dynamic state estimation, frequency control, smart grids, micro-grids, demand response, load shedding, and power system protection. He is included in the 2018 and 2019 Publons list of the top 1% best reviewer and researcher in the field of engineering. He was a recipient of the Outstanding Reviewer Award from *Energy Conversion and Management* Journal, in 2016, *ISA Transactions* Journal, in 2018, *Applied Energy* Journal, in 2019, and many other awards. He was also a recipient of the Best Young Researcher in the Arab Student Forum Creative among 61 researchers from 16 countries at Alexandria University, Egypt, in 2011. He has also performed more than 600 reviews for high prestigious journals, including IEEE TRANSACTIONS ON INDUSTRIAL INFORMATICS, IEEE TRANSACTIONS ON INDUSTRIAL ELECTRONICS, *Energy Conversion and Management*, *Applied Energy*, and *International Journal of Electrical Power & Energy Systems*.

• • •